NASA CR-72261

INVESTIGATION OF THE FLAME STRUCTURE OF A THERMALLY UNSTABLE FUEL

BY

S. HERSH, B.R. LAWVER, R.J. HOFFMAN, AND B.P. BREEN

FINAL REPORT

PREPARED FOR

NATIONAL AERONAUTICS AND SPACE ADMINISTRATION

CONTRACT NO. NAS 7-442

JUNE 1967

DYNAMIC SCIENCE
A DIVISION OF MARSHALL INDUSTRIES
MONROVIA, CALIFORNIA

NOTICE

Requests for copies of this report should be referred to:

National Aeronautics and Space Administration
Office of Scientific and Technical Information
Attention: AFSS-A
Washington, D. C. 20546

CR-72261

DS-SN81B

FINAL REPORT

INVESTIGATION OF THE FLAME STRUCTURE OF A THERMALLY UNSTABLE FUEL

By Stuart Hersh, B. R. Lawver, R. J. Hoffman, and B. P. Breen

prepared for

NATIONAL AERONAUTICS AND SPACE ADMINISTRATION

30 June 1967

CONTRACT NAS 7-442

Technical Management

NASA Lewis Research Center
Cleveland Ohio
Chemistry and Energy Conversion Division
Richard J. Priem
Charles E. Feiler

DYNAMIC SCIENCE
A Division of Marshall Industries
1900 Walker Avenue
Monrovia, California

FOREWORD

This final report documents the work performed at the Dynamic Science Division of Marshall Industries under NASA Contract Number NAS7-442, relating to the description of the flame structure of thermally unstable fuels. At Dynamic Science, this work was assigned the project number SN-81 B & C. Two additional reports will be published under this NASA contract which will describe the work performed under Dynamic Science project number SN-81 A and SN-81 D.

All phases of this contract were monitored by Dr. Charles Feiler and Dr. Richard Priem of NASA-Lewis Research Center. At Dynamic Science, Dr. B. P. Breen was Program Manager of the total contract (NAS7-442). Mr. R. J. Hoffman acted as Technical Manager of the work reported in this report (SN-81 B & C). The analytical model (Appendix A) was developed by Mr. S. Hersh, Mr. B. R. Lawver designed and constructed the experimental equipment and the experiments were conducted by Mr. Hersh and Mr. Lawver. Dr. E. W. Nadig was responsible for the physical properties, Appendix B.

Thanks are expressed to Mr. John White, Mr. Wm. Irwin, and Mr. Frank Cummings for their assistance in constructing and operating the experimental equipment.

ABSTRACT

The results of an investigation of the hydrazine/nitrogen tetroxide droplet flame are reported. The results of the experimental work are the temperature and stable species concentration profiles. It is concluded that a hydrazine decomposition flame exists at the droplet surface causing a large temperature gradient which results in much higher burning rate than found for thermally stable fuels.

CONTENTS

SUMMARY

The flame structure of a 2500 micron hydrazine drop burning in nitrogen tetroxide was determined experimentally by measuring the temperature and specific concentrations at a plane 90^{o} from the stagnation point. The hydrazine drop diameter was maintained constant by suspending it on the end of a water cooled hypodermic needle attached to a constant flow rate syringe. N_2O_4 was fed into the burner, establishing a thermal convective flow field around the drop. The flame was probed with a shielded 0.002 inch platinum-platinum/10% rhodium thermocouple as well as a concentration sampling probe. Both an "outer" and an "inner flame" were visually observable. The locations of these "flames" do not coincide with the high temperature points in the drop combustion zone, and therefore are not true flames but regions of strong visible radiation.

The experiments indicate that hydrazine decomposes very close to the liquid drop surface producing a steep temperature gradient which controls the burning rate. Although not proven conclusively, the zone between the drop and the inner flame appears to consist primarily of hydrazine decomposition products.

INTRODUCTION

An understanding of the processes by which a liquid fuel drop is vaporized and burned in the presence of an oxidizing media is essential to predicting the combustion process within a liquid rocket engine. In the course of an investigation of the rate of burning of a hydrazine drop in an atmosphere of N_2O_4/NO_2, it was found that conventional methods of treating droplet burning did not give results in agreement with the experiment.

In an attempt to account for the difference in burning rate of an exothermic fuel drop (N_2H_4) and an endothermic drop (Heptane), experimental hydrazine decomposition rate data were applied to the prediction of combustion within the low velocity regions of a rocket engine (Ref. 1). While this approach showed promise of predicting correct burning rate and engine performance for the hydrazine family of fuels, it appeared appropriate, in view of the absence of similar studies, to investigate the two flame nature of hydrazine/nitrogen tetroxide burning in detail.

The objective of this work was thus to provide a description of the oxidiation of thermally unstable rocket fuels so that model of burning rate within a combustion chamber could be developed.

SYMBOLS

D_{ij} = the binary diffusion coefficients of i^{th} specie into each of the other species(cm^2/sec)

H_i = the enthalpy of the i^{th} species at temperature T. (cal/mole)

H_{fo} = the enthalpy of the fuel at its initial conditions (cal/mole)

K = thermal conductivity(cal/cm sec °C)

K_m = equilibrium constant for the m^{th} reaction

ℓ = index for atomic species (e.g. ℓ=1 indicates the 1st atomic specie)

P_i = partial pressure of the i^{th} specie ($P_i/P = x_i$)

R = gas constant

s = total number of atomic species

W_f = the fuel burning rate in (moles/second)

W_i = rate of transport of the i^{th} chemical species in (moles/second)

x_i = the mole fraction of the i^{th} specie (moles i/moles$_{(mix)}$)

$\alpha_{i,\ell}$ = the number of ℓ atoms in the i^{th} specie

$\alpha_{f,\ell}$ = the number of ℓ atoms in a fuel molecule.

$\beta_{i,m}$ = stoichiometric coefficients for the reactants of the m^{th} reaction

$\epsilon_{i,m}$ = stoichiometric coefficients for the products of the m^{th} reaction

ν = total number of chemical species

DISCUSSION

Although semi-analytical models for the determination of the burning rate of thermally stable fuel drops have been developed (Ref. 2), an analytical determination of the burning rate of a thermally unstable drop, such as hydrazine has not been achieved.

Liquid hydrazine burning in NTO exhibits two visibly discrete "flames" (Figure 1). Initial studies ascribed the "inner flame" to the energy released by hydrazine decomposition, the "outer flame" being the region of oxidation of the decomposition products.

As part of a program to gain understanding of the processes underlying the hydrazine/NTO flame structure an analytical model which could be used to determine the N_2H_4 burning rate under several simplifying assumptions was formulated (Appendix A) and experimental studies of the flame properties were conducted.

The transport properties required by the analysis, consisting of both measured values and approximate formulas where no experimental data was available, are compiled in Appendix B. This information is of a general nature and is therefore of use for any analysis for which information of this type is necessary.

Two series of experimental tests were conducted. Both series utilize the same basic equipment, the difference being in the instrumentation used to measure the flame parameters. Temperature profiles from the ambient atmosphere to the drop surface were obtained using a thermocouple probe while individual specie concentrations in the hydrazine-nitrogen tetroxide flame were determined from a mass spectrometric analysis of samples withdrawn from the flame with a sampling probe.

Hydrazine was chosen for use in these tests because it is the basic ingredient in the most widely used thermally unstable fuel and the result would have the greatest practical application. Burning droplet tests were run with propellant grade hydrazine burning the oxidizers, nitrogen tetroxide, oxygen, air, and oxygen/nitrogen mixtures. Temperature profiles were measured with all of these oxidizers, however, concentration probing was done only for the nitrogen tetroxide oxidizer.

APPARATUS AND PROCEDURE

Objectives. - The purpose of these experiments was to measure the flame structure of a hydrazine droplet burning in nearly stagnant nitrogen tetroxide vapor. The flame structure was defined by measuring the temperature profile and chemical species concentration in the free convective flame surrounding a constant diameter hydrazine droplet. Tests were also conducted with hydrazine burning in oxygen/nitrogen mixtures to measure the effect of the oxidizer concentration on the flame structure.

These tests were conducted with propellant grade hydrazine and nitrogen tetroxide. The oxygen and nitrogen gases were supplied from standard gas cylinders.

The Burner. - The tests were conducted with the burner apparatus* shown in Figure 2. Basically the burner consists of a test section which permits observation of the combustion and the related propellant feed systems. The burner is designed such that either liquid fuel droplets or gaseous fuels can be burned in gaseous oxidizers. A flow schematic of the burner propellant feed system is shown in Figure 3.

The droplet flame is produced by suspending the fuel droplet from a water cooled hypodermic needle in the burner test section. The fuel is fed from a syringe into the suspension needle with a variable speed syringe drive. The droplet diameter can be maintained constant by proper adjustment of the syringe drive.

The fuel droplet suspension needle is shown in Figure 4. It is a 0.010" O.D. (0.005" I.D.) tube surrounded by two larger concentric tubes through which water is circulated. The water provides cooling of the exposed proportion of the small needle, to prevent boiling and thermal decomposition of the fuel within the needle. The oxidizing gases are fed into the burner through an injector tube located in the burner base plate. The oxidizer flow rates are controlled with calibrated sonic orifices, by regulating the orifice upstream pressures. Oxygen is fed to the burner orifice through a pressure regulator mounted on the supply bottle. The N_2O_4 vapor is generated by electrically heating the storage tanks and supply lines. The N_2O_4 vapor temperature and flowrate are controlled by regulating the heater current. The N_2O_4 flowrate is also measured with a calibrated sonic orifice.

*This burner was designed and built under Contract AF 04(611)-11616.

The burner test section has opposing pyrex windows for observing and photographing the flames. The combustion products are removed from the burner tube with an air driven ejector mounted to the burner top plate.

Temperature Probe. - The temperature probe is illustrated in Figure 5. This probe consists of 0.002" diameter platinum/platinum-10% rhodium thermocouple wires mounted in a small ceramic insulator encased in a stainless steel sheath. The steel sheath protects the exposed wires from the hot combustion gases when the probe is fully submerged into the flame, as is illustrated in Figure 7.

A 0.010" diameter platinum/platinum-10% rhodium thermocouple without the steel sheath was used for the initial probing of the N_2H_4 flame. These tests indicated that heat conducted along the thermocouple leads from the exposed portion of the wires caused erroneous temperature measurements, therefore, it was necessary to provide a steel sheath. In addition the response of the larger thermocouple was not satisfactory. To improve the response time an attempt was made to construct thermocouples with 0.001" diameter wires, however this proved to be too time consuming to be warranted. The response of the 0.002" diameter thermocouple is on the order of 40 milliseconds.

The thermocouples were calibrated by immersing the probe in compounds with known melting point temperatures. The calibration data points are shown in Figure 6 along with a plot of the standard calibration for thermocouples obtained from Reference 3. The good agreement between the observed and standard calibrations encouraged the use of the latter in the higher temperature range where calibration measurements were not made.

The thermocouple probe is traversed through the droplet flame with a variable speed electric motor drive mechanism as shown schematically in Figure 7. The thermocouple position is indicated on an oscilloscope by using the signal from a 5000 Ω linear potentiometer to drive the oscilloscope horizontal sweep. The thermocouple output voltage is applied to the oscilloscope vertical amplifier input, providing direct temperature versus distance profile throughout the flame region. The temperature profile is recorded by photographing the oscilloscope screen with a bezel mounted Poloroid camera.

Concentration Probe. - The concentration sampling technique described in Reference 4, was used to measure the chemical species concentrations in the N_2H_4 flames. The technique consists of kinetically freezing the reacting gases by drawing them through a very small supersonic nozzle into a vacuum environment. The rapid expansion quenches the reactions, thus preserving the stable chemical species for subsequent analysis.

The concentration sampling probe is a 6mm O.D. quartz tube with 1mm walls, drawn to a fine point at the sampling end to minimize the flame disturbance. The nozzle throat diameter is 0.002 inches in diameter which gives an expansion ratio of 6200/1. The inlet area ratio is 300/1. Based on a flame gas velocity of 6-10 ft/sec, the nozzle residence time is approximately 40 μ sec.

The sampling system is shown in Figure 8. The gas samples were collected in bottles and then analyzed on a Hitachi Perkin-Elmer mass spectrograph.

The mole fractions were calculated from the relationship

$$x_i = \frac{P_i}{P_T}$$

where

x_i = mole fraction of species i

P_i = partial pressure of species i

P_T = total pressure of sample

The partial pressures are determined from the magnitude of the mass peaks measured with the mass spectrograph. The partial pressures are found from the relationship

$$h_m = \sum_i^n K_i^m P_i$$

where h_m = measured peak height of mass number (m)

K_i = sensitivity of species (i) to mass number (m)

There is one equation for each mass number and the problem then is the solution of a system of simultaneous equations. The number of equations is equal to the number of species involved. To simplify the data reduction, these equations were programmed on a CDC 3600 computer. The input consists of the measured mass peak heights of the species of interest and the sensitivity factors. The output is the species mole fractions.

Analysis of the mass peaks for the hydrazine/NTO flame indicated that the mass numbers of interest are,

Mass Number	Species
2	H_2
17	NH_3
18	H_2O
28	N_2
29	N_2H_4
30	NO
32	O_2
44	N_2O
46	NO_2

The mass number 29 was used for the hydrazine to distinguish it from oxygen, mass number 32. The hydrazine exhibits a 29 peak that is 43% of its 32 peak, also it exhibits a strong peak at mass number 31. The above mass numbers and species were used in determining the hydrazine/NTO flame structures.

Experimental Results

Temperature Profiles. - A typical temperature profile for a hydrazine-nitrogen tetroxide flame is shown in Figure 9. The temperature begins to rise before the "outer flame" is reached and rises to a peak between the "inner" and "outer flame." This peak temperature corresponds to a blue region which is visually observable but does not appear in the flame photographs. Attempts to use film with a greater spectral sensitivity in the blue region than the Polaroid color film normally used also failed to reproduce this region. The temperature decreases smoothly from its maximum, through the "inner flame," to a relatively high value close to the drop surface. It should be noted that the locations of the visible "flames" do not coincide with the high temperature points. Thus what have been denoted as the "inner" and "outer flames" are not true flames but regions of strong visible radiation.

The shape of this temperature profile, in particular the high temperature close to the drop surface would indicate that hydrazine decomposition had occurred at the droplet surface. To further examine this behavior, hydrazine droplets were burned in oxygen-nitrogen atmospheres at various O_2-N_2 concentrations. A hydrazine-air profile is shown in Figure 10. As can be seen, both the maximum and drop surface temperatures, are less than that obtained for the hydrazine-NTO system, (Figure 9).

The O_2-N_2 concentrations were varied over a small range by varying the pressures upstream of the sonic orifices. Figures 11a and b, are temperature profiles for hydrazine burning in oxygen-nitrogen atmospheres of different O_2-N_2 concentrations, Figure 11a being at a higher value of O_2-N_2 ratio. The temperature profile shown in Figure 12 was obtained by reducing the oxygen concentration until the only visual evidence of burning was a halo-type glow close to the drop surface (Figure 13). Under this condition the actual temperatures were lower than those for the other cases but the steep gradient at the drop surface is still evident. The change in distance scale should be noted. Also it should be noted that the temperature near the drop surface with N_2H_4/air is not much higher than the maximum temperature of the halo flame.

To verify that the temperature profiles obtained for hydrazine were functions of the hydrazine itself and not related to the experimental procedures or equipment, the flame surrounding a heptane drop was also probed. Heptane was selected because of its endothermicity. Therefore, if the temperature gradient at the surface of the hydrazine drop is due to hydrazine decomposition, it would be expected that the profile obtained for the heptane drop would not exhibit this steep gradient. Figure 14a is the temperature profile obtained for heptane. As can be seen, the temperature rises to a peak and then decreases to the droplet boiling temperature. Figure 14b shows that two visible "flames" are also present when heptane is burned in nitrogen tetroxide. Other investigators, for example, Wharton, Miller, et al, (Ref. 5 and 6) have also observed a dual reaction zone in premixed n-butane-NO_2 flames. These results suggest that the two "visible flames" are associated with the oxidizer while two real flames are found only for hydrazine. The combustion of hydrazine with any oxidizer will be a two flame structure consisting of decomposition at the droplet surface and the oxidation of the decomposition products.

<u>Concentration Profiles.</u> - The concentration data taken at several positions in the flame are plotted versus reduced radius in Figure 15. It is noted that hydrazine was not found in measurable quantities. There is some question as to whether this is due to the nonexistence of hydrazine in the flame or to hydrazine decomposition in the sampling probe.

Figure 15 also indicates that the outer flame consists of the decomposition of NO_2 to NO and O_2. The mole fractions of NO and O_2 decrease as the inner flame is approached.

The fact that the decrease in NO occurs in the region where the temperature reaches a maximum is in agreement with the results of Reference 5. That investigation demonstrated that the maximum temperature

in an n-butane-NO_2 flame was due to the energy release associated with the decomposition of NO. At the inner flame boundary the oxidizer concentrations drop sharply to very small amounts.

Several phenomena which relate to the accuracy of the sampling results were observed. It was found that ammonium nitrate was collected in the probe throat at the yellow inner flame boundary. This problem prevents an accurate description of the inner flame composition being made by direct sampling. It is not apparent whether the ammonium nitrate is formed in the probe or is precipitated from the flame. The formation of the ammonium nitrate in the probe would require very fast reaction rates at low temperature. Ammonium nitrate is a stable product of the room temperature hypergolic reaction between NH_3 and NO_2, therefore, it is conceivable that it may also be an intermediate of the high temperature reaction.

The relative amounts of nitrogen were larger than they should have been, but this may be due to contamination from the probe purge system.

CONCLUSIONS

The facts that, all tests conducted with hydrazine indicate the presence of a steep temperature gradient near the drop, and that this property is associated only with hydrazine droplets, lead to the conclusion that hydrazine decomposition occurs at or very near the drop surface. This conclusion appears to be further verified by the concentration profiles obtained with the sampling probe. The failure to detect any hydrazine in the flame especially in the region near the drop surface, when viewed in the light of the temperature profiles, is a further indication of hydrazine decomposition at or close to the drop surface.

The results of these experiments indicate that at low Reynolds number the dominant process controlling the hydrazine burning rate is hydrazine decomposition, since this mechanism determines the temperature gradient at, and therefore the heat transfer to, the droplet surface. The existence of the decomposition flame at the drop surface causes hydrazine to have a significantly higher burning rate than thermally stable fuels such as heptane.

APPENDIX A

ANALYTICAL VAPOR PHASE DECOMPOSITION MODEL

Analytical Model

Derivation of Equations. - The analysis of the burning of a drop of hydrazine in a nitrogen tetroxide atmosphere has been formulated in a manner similar to that described by Coffin and Brokaw (Ref. 2), in which equilibrium chemistry was assumed. As in Reference 2, the problem is set up for a general fuel-oxidizer combination with the particular system under examination determining the necessary physical properties.

The equations describing the processes occurring in the region between the fuel drop surface and the ambient oxidizer atmosphere are:

Conservation of Mass

$$W_\ell = \sum_{i=1}^{\nu} \alpha_{i,\ell} W_i \qquad \ell = 1, \ldots . s$$

W_i = Rate of transport of the i^{th} chemical species in (moles/sec)

ℓ = Index for atomic species. (e.g. ℓ=1 indicates the 1st atomic specie)

$\alpha_{i,\ell}$ = The number of ℓ atoms in the i^{th} specie

s = Total number of atomic species

ν = Total number of chemical species

This equation expresses the fact that the transport of the ℓ^{th} atomic species through any surface is equal to the sum of the contributions due to the transport of chemical species containing ℓ atoms. Since there is no sink in the system the net transport of oxidizer atoms is zero. However, there is a net production of fuel atoms since the drop is a fuel source. Therefore

$$W_\ell = \alpha_{f,\ell} W_f$$

W_f = the fuel burning rate in (moles/second) and $\alpha_{f,\ell}$ = the number of ℓ atoms in a fuel molecule.

or

$$\sum_{i=1}^{\nu} \alpha_{i,\ell} W_i = \alpha_{f,\ell} W_f \qquad \ell = 1, \ldots . s$$

which describes the conservation of atoms in the systems.

Energy Equation

$$W_f H_{fo} - \sum_{i=1}^{\nu} W_i H_i = -4\pi r^2 K \frac{dT}{dr}$$

H_i = The enthalpy of the i^{th} species at temperature T.

H_{fo} = The enthalpy of the fuel at its initial conditions

K = Thermal conductivity

Diffusion Equations

The equations describing the diffusion of the i^{th} species are obtained from the general diffusion equations (Eqn. 8-1-3 of Ref. 7) by neglecting external forces, pressure gradients, and thermal diffusion. In addition it is also assumed that each specie i obeys the ideal gas law and that the binary diffusion coefficients of the i^{th} specie (D_{ij}) into each of the other species are equal, i.e. $D_{ij} = D_i$. Under these conditions the diffusion equations can be put in the form (Ref. 2).

$$W_i = -4\pi r^2 \frac{P}{RT}\left(D_i \frac{dx_i}{dr} + \frac{x_i}{x_\nu}\sum_{j=1}^{\nu-1} D_j \frac{dx_j}{dr}\right) + \frac{x_i}{x_\nu} W_\nu \qquad i = 1,\ldots \nu-1$$

R = Gas constant

x_i = The mole fraction of the i^{th} specie ($\frac{\text{Moles } i}{\text{Moles}_{(mix)}}$)

For a ν component gas there are $\nu-1$ independent transport rates.

Chemistry Equations

If the transport rates are much slower than the chemical rates the burning process can be considered to occur under equilibrium conditions. For a ν component system there are $\nu-s$ independent equilibrium relationships among the chemical species.

These relations are of the form $$K_m = \frac{\prod_i^{\nu} p_i^{\epsilon_{i,m}}}{\prod_i^{\nu} p_i^{\beta_{i,m}}}$$

p_i = Partial pressure of the i^{th} specie ($\frac{p_i}{P} = x_i$)

K_m = Equilibrium constant for the m^{th} reaction.

$\epsilon_{i,m}$ = Stoichiometric coefficients for the products of the m^{th} reaction

$\beta_{i,m}$ = Stoichiometric coefficients for the reactants of the m^{th} reaction.

If the transport and chemical rates are comparable, the relationships between the gas components must be determined by finite rate chemistry.

Normalization Equation

$$\sum_{i=1}^{\nu} x_i = 1$$

That is, the sum of the mole fractions is unity.

In summary, there are s conservation of mass equations, one energy equation, $\nu-1$ diffusion equations, ν -s chemical equations, and a normalization equation for a total of $2\nu+1$ equations. There are $\nu+1$ unknown W's (W_i $i = 1, \ldots . \nu$ and W_f) and ν unknown fractions (x_i $i = 1, \ldots . \nu$). Thus there are $2\nu+1$ unknowns and $2\nu+1$ equations and the problem is solvable in principle.

Since there are ν W's and $\nu-1$ diffusion equations one of the mass conservation equations must be used to determine the ν^{th} W. The conservation equations are

$$\sum_{i=1}^{\nu} \alpha_{i,\ell} W_i = \alpha_{f,\ell} W_f \qquad \ell = 1, \ldots . s$$

Select ℓ for which $\alpha_{f,\ell} \neq 0$

Designate this value of ℓ as $\lambda 1$.

Then

$$\sum_{i=1}^{\nu-1} \alpha_{i,\lambda 1} W_i + \alpha_{\nu,\lambda 1} W_\nu = 0$$

or

$$W_\nu = -\frac{1}{\alpha_{\nu,\lambda 1}} \sum_{i=1}^{\nu-1} \alpha_{i,\lambda 1} W_i$$

Substituting for W_i from the diffusion equation and solving for W_ν

$$W_\nu = \frac{\frac{4\pi r^2 P}{RT} \sum_{i=1}^{\nu-1} \alpha_{i,\lambda 1} \left(D_i \frac{dx_i}{dr} + \frac{x_i}{x_\nu} \sum_{i=1}^{\nu-1} D_j \frac{dx_i}{dr} \right)}{\alpha_{\nu,\lambda 1} + \sum_{i+1}^{\nu-1} \alpha_{i,\lambda 1} \frac{x_i}{\nu}}$$

Therefore

$$-W_i = 4\pi r^2 \frac{P}{RT} \left\{ \left(D_i \frac{dx_i}{dr} + \frac{x_i}{x_\nu} \sum_{j=1}^{\nu-1} D_j \frac{dx_j}{dr} \right) - \frac{\frac{x_i}{x_\nu} \sum_{i=1}^{\nu-1} \alpha_{i,\lambda 1} \left(D_i \frac{dx_i}{dr} + \frac{x_i}{x_\nu} \sum_{j=1}^{\nu-1} D_j \frac{dx_j}{dr} \right)}{\alpha_{\nu,\lambda 1} + \sum_{i=1}^{\nu-1} \alpha_{i,\lambda 1} \frac{x_i}{x_\nu}} \right\}$$

In order to eliminate all the W's from the energy equation a second mass conservation equation is used to express W_f in terms of the W_i's. Select ℓ for which $\alpha_{f,\ell} \neq 0$. Designate this value of ℓ λ_2. The $\ell = \lambda_2$ conservation equation gives

$$W_f = \frac{1}{\alpha_{f,\lambda 2}} \sum_{i=1}^{\nu} \alpha_{i,\lambda 2} W_i$$

Substituting into the energy equation gives

$$\frac{H_{fo}}{\alpha_{f,\lambda 2}} \sum_{i=1}^{\nu} \alpha_{i,\lambda 2} W_i - \sum_{i=1}^{\nu} W_i H_i = -4\pi r^2 K \frac{dT}{dr}$$

Rearranging

$$\sum_{i=1}^{\nu-1} \left(\frac{\alpha_{i,\lambda 2}}{\alpha_{f,\lambda 2}} H_{fo} - H_i \right) W_i + \left(\frac{\alpha_{\nu,\lambda 2}}{\alpha_{f,\lambda 2}} H_{fo} - H_\nu \right) W_\nu = -4\pi r^2 K \frac{dT}{dr} \tag{1}$$

The S-2 remaining conservation equations are

$$\sum_{i=1}^{\nu} \alpha_{i,\ell} = \frac{\alpha_{f\ell}}{\alpha_{f,\lambda 2}} \sum_{i=1}^{\nu} \alpha_{i,\lambda 2} W_i \qquad \begin{array}{l} \ell = 1, \ldots s \\ \ell \neq \lambda_1, \lambda_2 \end{array}$$

$$\sum_{i=1}^{\nu} \left(\alpha_{i,\ell} - \frac{\alpha_{f,\ell}}{\alpha_{f,\lambda 2}} \right) W_i = 0$$

$$\sum_{i=1}^{\nu-1} \left(\alpha_{i,\ell} - \frac{\alpha_{f,\ell}}{\alpha_{f,\lambda 2}} \alpha_{i,\lambda 2} \right) W_i + \left(\alpha_{\nu,\ell} - \frac{\alpha_{f,\ell}}{\alpha_{f,\lambda 2}} \alpha_{\nu,\lambda 2} \right) W_\nu = 0 \tag{2}$$

Equations (1) and (2) are of the form

$$\sum_{i=1}^{\nu-1} A_i W_i + B W_\nu = C \tag{3}$$

Examining the terms in the above equation separately gives for the first term

$$-\frac{RT}{4\pi r^2 P}\sum_{i=1}^{\nu-1} A_i W_i = \sum_{i=1}^{\nu-1} A_i D_i \frac{dx_i}{dr} + \sum_{i=1}^{\nu-1} A_i \frac{x_i}{x_\nu}\left(\sum_{j=1}^{\nu-1} D_j \frac{dx_j}{dr}\right)$$

$$-\frac{1}{S}\sum_{i=1}^{\nu-1} A_i \frac{x_i}{x_\nu}\sum_{i=1}^{\nu-1} \alpha_{i,\lambda 1} D_i \frac{dx_i}{dr} - \frac{1}{S}\sum_{i=1}^{\nu-1} A_i \frac{x_i}{x_\nu}\sum_{i=1}^{\nu-1} \alpha_{i,\lambda 1}\frac{x_i}{x_\nu}\sum_{j=1}^{\nu-1} D_j \frac{dx_j}{dr}$$

where

$$S = \alpha_{\nu,\lambda 1} + \sum_{i=1}^{\nu-1} \alpha_{i,\lambda 1}\frac{x_i}{x_\nu}\ .$$

This relation can be rearranged into the following form

$$-\frac{RT}{4\pi r^2 P}\sum_{i=1}^{\nu-1} A_i W = \sum_{i=1}^{\nu-1}\left\{A_i - \frac{\alpha_{i,\lambda 1}}{S}\sum_{i=1}^{\nu-1} A_i \frac{x_i}{x_\nu} + \sum_{i=1}^{\nu-1} A_i \frac{x_i}{x_\nu}\left(1-\frac{1}{S}\sum_{i=1}^{\nu-1}\alpha_{i,\lambda 1}\frac{x_i}{x_\nu}\right)\right\} D_i \frac{dx_i}{dr}$$

The second term is

$$\frac{RT}{4\pi r^2 P} BW_\nu = \frac{B}{S}\sum_{i=1}^{\nu-1}\alpha_{i,\lambda 1} D_i \frac{dx_i}{dr} + \frac{B}{S}\sum_{i=1}^{\nu-1}\alpha_{i,\lambda 1}\frac{x_i}{x_\nu}\sum_{j=1}^{\nu-1} D_j \frac{dx_i}{dr}$$

$$= \frac{B}{S}\sum_{i=1}^{\nu-1}\left(\alpha_{i,\lambda 1} + \sum_{i=1}^{\nu-1}\alpha_{i,\lambda 1}\frac{x_i}{x_\nu}\right) D_i \frac{dx_i}{dr}$$

Therefore Equation (3) becomes

$$\sum_{i=1}^{\nu-1}\left[\left\{A_i + \sum_{i=1}^{\nu-1} A_i \frac{x_i}{d_\nu} - \left(B + \sum_{i=1}^{\nu-1} A_i \frac{x_i}{x_\nu}\right)\left[\frac{\alpha_{i,\lambda 1} + \sum_{i=1}^{\nu-1}\alpha_{i,\lambda 1}\frac{x_i}{x_\nu}}{\alpha_{\nu,\lambda 1} + \sum_{i=1}^{\nu-1}\alpha_{i,\lambda 1}\frac{x_i}{x_\nu}}\right]\right\} D_i \frac{dx_i}{dr}\right] = -\frac{CRT}{4\pi r^2 P}$$

For Equation (1) $\quad C = -\,4\pi r^2 K \dfrac{dT}{dr}$

For Equations (2) $\quad C = 0$

Substituting into the above equation gives

$$\sum_{i=1}^{\nu-1}\left[\left\{A_i + \sum_{i=1}^{\nu-1} A_i \frac{x_i}{x_\nu} - \left(B + \sum_{i=1}^{\nu-1} A_i \frac{x_i}{x_\nu}\right)\left[\frac{\alpha_{i,\lambda 1} + \sum_{i=1}^{\nu-1}\alpha_{i,\lambda 1}\frac{x_i}{x_\nu}}{\alpha_{\nu,\lambda 1} + \sum_{i=1}^{\nu-1}\alpha_{i,\lambda 1}\frac{x_i}{x_\nu}}\right]\right\}\delta_i \frac{dx_i}{dT}\right] = C' \qquad (4)$$

where $\delta_i = \frac{D_i}{KRT}$

For Equation (1)

$$A_i = \left(\frac{\alpha_{i,\lambda 2}}{\alpha_{f,\lambda 2}} H_{fo} - H_i \right)$$

$$B = \left(\frac{\alpha_{\nu,\lambda 2}}{\alpha_{f,\lambda 2}} H_{fo} - H_i \right)$$

$$C' = \frac{1}{P}$$

For Equations (2)

$$A_i = (\alpha_{i,\ell} - \frac{\alpha_{f,\ell}}{\alpha_{f,\lambda 2}} \alpha_{i,\lambda 2}) \qquad \ell = 1, \ldots . S$$

$$\ell \neq \lambda_1, \lambda_2$$

$$B = (\alpha_{\nu,\ell} - \frac{\alpha_{f,\ell}}{\alpha_{f.\lambda 2}} \alpha_{\nu,\lambda 2})$$

$$C' = 0$$

The chemical equilibrium relations are

$$K_m = \frac{\prod_i^{\nu} p_i^{\epsilon_{i,m}}}{\prod_i^{\nu} p_i^{\beta_{i,m}}}$$

Taking the temperature derivative of this equation gives

$$\frac{d}{dT} \prod_i^{\nu} p_i^{\epsilon_{i,m}} = K_m \frac{d}{dT} \prod_i^{\nu} p_i^{\beta_{i,m}} + \prod_i^{\nu} p_i^{\beta_{i,m}} \frac{dK_m}{dT}$$

But $\frac{d}{dT} \prod_i^{\nu} p_i^{\epsilon_{i,m}} = \prod_j^{\nu} p_i^{\epsilon_{j,m}} \sum_{i=1}^{\nu} \epsilon_{i,m} p_i^{-1} \frac{dp_i}{dT}$

Substituting and rearranging yields

$$\sum_{i=1}^{\nu} \left\{ \left[\epsilon_{i,m} \prod_j px_j^{(\epsilon_{j,m} - \beta_{j,m})} - K_m \beta_{i,m} \right] \frac{1}{x_i} \frac{dx_i}{dT} \right\} = \frac{dK_m}{dT} \qquad (5)$$

$$m = 1, \ldots \nu - S$$

Where the relationship between the partial pressure and the mole fraction, $x_i = p_i/p$, has been used.

It should be noted that Equations (5) provide ν-S relations between the x_i's. While these equations were derived for equilibrium chemistry and other chemical assumptions, e.g. finite rate kinetics, or arbitrary specification of x_i vs T, can be made, providing a set of ν-S independent relationships are obtained.

The normalization equation can also be differentiated to give

$$\sum_{i=1}^{\nu} \frac{dx_i}{dT} = 0 \tag{6}$$

Equations (4), (5), and (6) are respectively S-1, ν-S, 1, equations for a total of ν equations for the ν unknown x_i's.

The above equations can be numerically integrated to give x_i vs T for all the species. The mass conservation equations can then be used to obtain the spatial specie distribution from the drop to the ambient atmosphere.

Since the experimental programs described above indicated that the hydrazine burning rate was controlled by decomposition close to the drop surface the usefulness and applicability of an analytical model of this type toward the prediction of the burning rate was uncertain and a computer code was not developed.

APPENDIX B

PHYSICAL PROPERTIES

For use in the analytical hydrazine decomposition model, enthalpies, diffusion coefficients, and thermal conductivities are needed for the following chemical species: H_2, NH_3, N_2, H_2O, NO, NO_2, O_2, O, N, NH_4NO_3, and N_2H_4.

Enthalpies. - The enthalpies of H_2, NH_3, N_2, H_2O, NO, NO_2, O_2, O, and N are given in Reference (8) from 0° K to 6000° K. The enthalpies of N_2H_4 and NH_4NO_3 are not given but can be determined from the same NASA-Lewis program. However, apparently the program shows that N_2H_4 does not exist as such at any temperature since equilibrium calculations are involved.

Diffusion Coefficients. - Two suitable expressions are available for determining the coefficient of diffusion in a binary mixture.

Hirschfelder, Curtiss, and Bird, (Ref. 4) give the analytical expression

$$D_{12} = 0.0026280 \frac{\sqrt{T^3 (M_1+M_2)/2M_1M_2}}{p\,\sigma_{12}^2\,\Omega_{12}^{(1,1)*}(T_{12}{}^*)}$$

where

D_{12} = diffusion coefficient

p = pressure

$\sigma_{12} = \frac{\sigma_1+\sigma_2}{2}$

σ_1, σ_2 = molecular diameters of species 1 and 2

T = temperature

M_1, M_2 = molecular weights of species 1 and 2

$\Omega_{12}^{(1,1)*}$ = integral parameter, approximately equal to 1.

T_{12}^* = overall reduced temperature between the two species

Another suitable expression for estimating the diffusion coefficient between species 1 and 2 is the empirical Gilliland (Ref. 9) expression

$$D = 0.0043 \frac{T^{3/2}}{p(V_A^{1/3} + V_B^{1/3})^2} \sqrt{\frac{1}{M_1} + \frac{1}{M_2}}$$

where

D = diffusivity, cm^2/sec

T = temperature, $^{\circ}K$

p = pressure atm

$M_1 M_2$ = molecular weights of gases

V_A, V_B = molecular volumes at the normal boiling points, cc/g-mole

The molecular volume can be calculated from the molecular weight and the density of the substance at the boiling point. If the density at the boiling point is unknown, the molecular volume can be calculated from the sum of the atomic volumes. The atomic volumes are given in Reference 10.

Thus, if the molecular diameters are given (some are given in Ref. 7) the more exact Hirschfelder, Curtiss, and Bird equation can be used. If the molecular diameters are unknown, the Gilliland equation can be used. Either equation will give a reasonable estimate of the diffusion coefficient in a binary mixture.

Since a binary gas mixture is assumed in use of the equations, in the actual multicomponent case the diffusion coefficient can be obtained from a mass weighted average of the properties of the remaining species into which the i^{th} specie is diffusing. If the specie diffuses into a mixture containing a large amount of one component with respect to the others in the mixture (i.e. approaching an overall binary mixture between the specie and the remaining material) the calculation will be reasonably accurate. The error involved if the overall mixture (specie diffusing plus the remaining materials) is not a binary mixture is not known at this time. It should be mentioned, that in a binary gas mixture, the dependence of the diffusion coefficient on composition is only slight.

Thermal Conductivities. - Since only limited experimental thermal conductivity data is available, it is necessary to use a theoretical expression to determine the thermal conductivity.

The thermal conductivity of a substance can be reasonably estimated from an analytical expression given by Hirschfelder, Curtiss, and Bird, (Ref. 7).

$$k = 1989.1 \times 10^{-7} \frac{\sqrt{T/M}}{\sigma^2 \, \Omega^{(2,2)*}(T^*)} \left(\frac{4}{15} \; \frac{C_p}{R} + \frac{1}{3} \right)$$

where

k	= thermal conductivity
T	= temperature
M	= molecular weight
σ	= molecular diameter
$\Omega^{(2,2)*}$	= integral parameter, approximately equal to 1.
C_p	= heat capacity
R	= universal gas constant
T^*	= reduced temperature

As used in the model, the thermal conductivity, k, is included because of a comparison with heat conduction. Therefore, k represents an overall constant value. In this analysis, the thermal conductivity will be determined from a mass weighted average of the thermal conductivities of the respective species. The closer one specie comes to being present in a large amount, the more accurate the use of the mass weighted average thermal conductivity will be.

Whenever possible experimentally determined values of the thermal conductivity of the substance should be used.

High temperature thermal conductivity data (3000-4700°F) is available in Reference 11. Figure 16 shows experimental results obtained from Reference 11 in addition to results from Reference 12 (indicated by the broken line).

The following low temperature experimental thermal conductivity (k) data is available for all of the species except O, N, NH_4NO_3, and N_2H_4.

	Temperature,	k $\frac{\text{calories}}{\text{cm sec °C}}$	Reference
NH_3	- 57.6°C	3.82	13
	0	5.135	13
	100	7.09	13
N_2	-191.4	1.829	13
	- 78.4	4.305	13
	0	5.68	13
	100	7.18	13

	Temperature	k $\frac{\text{calories}}{\text{cm sec}^\circ\text{C}}$	Reference
H_2	-252.2°C	3.22	13
	- 78.4	30.65	13
	0	39.60	13
	100	49.94	13
H_2O(g)	46	4.580	13
	100	5.510	13
NO (g)	- 71.4	4.160	13
	0	5.55	13
NO_2(g)	55	8.88	13
O_2	-191.4	1.721	13
	- 78.4	4.292	13
	0	5.70	13
	100	7.427	13
	80°K	1.701	14
	90	1.930	14
	100	2.159	14
	110	2.387	14
	120	2.614	14
	130	2.840	14
	140	3.064	14
	150	3.287	14
	160	3.508	14
	170	3.728	14
	180	3.946	14
	190	4.162	14
	200	4.375	14
	210	4.584	14
	220	4.790	14
	230	4.993	14
	240	5.194	14
	250	5.392	14
	260	5.586	14
	270	5.780	14
	273.1	5.839	14
	280	5.970	14
	290	6.159	14
	293.1	6.218	14
	298.1	6.314	14
	300	6.350	14

	Temperature	k $\frac{\text{calories}}{\text{cm sec}^\circ\text{C}}$	Reference
O_2	310°K	6.547	14
	320	6.748	14
	330	6.954	14
	340	7.164	14
	350	7.378	14
	360	7.594	14
	370	7.812	14
	380	8.033	14

Thermal Decomposition of Hydrazine. - In connection with the model, information on the thermal decomposition of hydrazine is desired. Although there are discrepancies in the literature, the following information is considered significant.

Thomas (Ref. 15) shows that hydrazine decomposes according to two consecutive overall reactions at 20 atm total pressures

$$3H_2H_4 \rightarrow 4NH_3 + N_2 + 80.15\text{Kcal} \qquad \text{(I)}$$

$$4NH_3 \rightarrow 2N_2 + 6H_2 - 44.00\text{ Kcal} \qquad \text{(II)}$$

The overall decomposition reaction is

$$3N_2H_4 \rightarrow 4(1-x)NH_3 + (1+2x)N_2 + 6xH_2 + (80.15-44.00x)\text{Kcal}$$

where x = the fraction of NH_3 decomposed.

Ammonia (NH_3) is only negligibly dissociated for temperatures below 400°K. As the temperature is raised above 400°K, NH_3 decomposes with the decomposition becoming complete at 800°K. Experimental results show that the decomposition reaction of NH_3 (II) is slower than reaction I. Hence, if the decomposition (I) occurs in the order of milliseconds, it then might be reasonable to assume that only part of the NH_3 could decompose.

Lucien (Ref. 16) carried out thermal decomposition studies of hydrazine in the ranges of 175° to 250° C and 300 to 430 psi. He found that the decomposition went according to

$$3N_2H_4 \rightarrow 4(1-x)NH_3 + (1+2x)N_2 + 6xH_2$$

where $x = 0.017$ at 222° C and 300 psi

$= 0.034$ at 250° C and 430 psi

The calculated activation energy was about 73Kcal per mole which is greater by a factor of two than other reported values. The rate of decomposition decreased with pressure over the range studied.

Eberstein and Glassman (Ref.17) studied hydrazine decomposition. The rate constant for hydrazine was found to be

$$k = 10^{10.33} \exp(-36{,}170/RT) \sec^{-1}$$

The stoichiometry observed was

$$N_2H_4 \rightarrow 0.9\,NH_3 + 0.5N_2 + 0.6\,H_2$$

The disagreements in the literature may indicate that the hydrazine decomposition mechanism changes with pressure and temperature.

REFERENCES

1. Breen, B. P. and M. R. Beltran, Steady State Droplet Combustion with Decomposition: Hydrazine/Nitrogen Tetroxide, AIChE Paper No. 35c, presented at 61st National Meeting (1967), also "Analysis of Liquid Rocket Engine Combustion Instability, AFRPL-TR-65-254, Dynamic Science, 1966.

2. Coffin, K. P. and R. S. Brokaw: A General System for Calculating Burning Rates of Particles and Drops and Comparison of Calculated Rates for Carbon, Boron, Magnesium, and Isooctane. NACA TN 3929, February 1957.

3. Handbook of Chemistry and Physics 30th Edition. Chemical Rubber Publishing Co., 1946.

4. Fristrom, R. M. and A. A. Westenberg,: Flame Structure, McGraw-Hill, Inc., New York 1965.

5. Wharton, W. W., T. D. Violett, and E. Miller: Sixth Symposium (International) on Combustion, New York, Reinhold Publ. Corp., 1957.

6. Miller, E. and H. Setzer,: Sixth Symposium (International) on Combustion, p. 164, New York, Reinhold Publ. Corp., 1957.

7. Hirschfelder, Joseph O., Charles F. Curtiss, and R. Byron R. Bird: Molecular Theory of Gases and Liquids. John Wiley & Sons, Inc., 1954.

8. McBridge, S. Heimel, J. G. Ehlers, and S. Gordon: Thermodynamic Properties to 6000°K for 210 Substances Involving the First 18 Elements. NASA SP-3001, 1963.

9. Gilliland: Industrial and Engineering Chemistry, 22, 1091, 1930.

10. Perry, John H.: Chemical Engineers Handbook, McGraw-Hill Publ. Co. p. 538, 1950.

11. Israel, S. L., T. D. Hawkins, and S. C. Hyman: Thermal Conductivity of Hydrogen from 2000° to 4700°F. NASA CR-403, March, 1966.

12. Mann, J. and N. Blais: Thermal Conductivity of Helium and Hydrogen at High Temperatures, LA-2316, Sept. 1959.

13. Lange, N.: Handbook of Chemistry, 1949, Seventh Edition, p. 1546.

14. Rand Corporation: Physical Properties and Thermodynamic Functions of Fuels, Oxidizers, and Products of Combustion - II Oxidizers. Rept. R-129, February, 1949.

15. Thomas, D. D.: California Institute Technology Propulsion Laboratory Progress Rept. 9-13, Sept. 1947.

16. Lucien, Harold W.: Thermal Decomposition of Hydrazine. Journal of Chemical and Engineering Data, p. 594, October 1961.

17. Eberstein, J. and I. Glassman: The Gas-Phase Decomposition of Hydrazine and its Methyl Derivatives, 10th Intl. Sym. on Comb., pp 365-374, 1965.

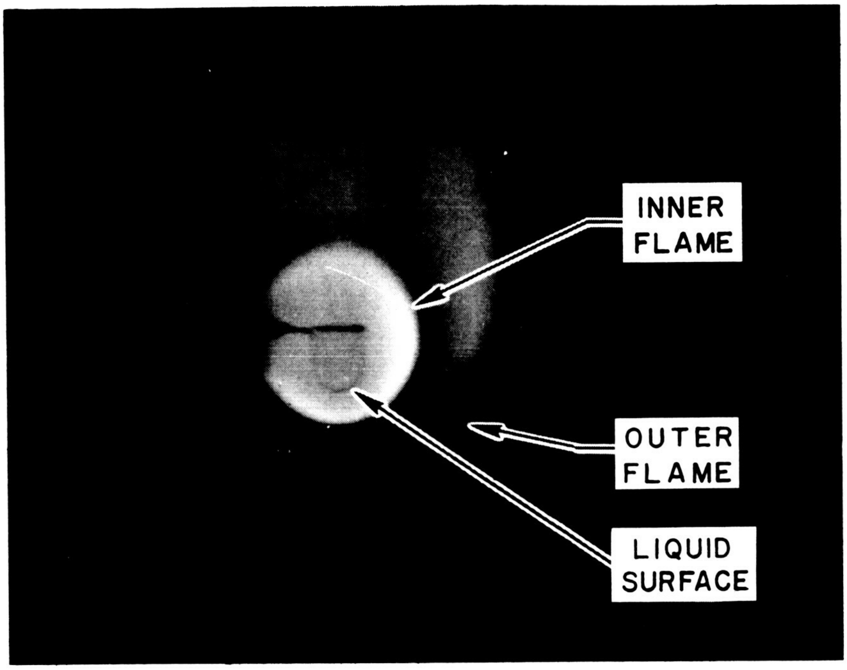

.FIGURE 1. HYDRAZINE / NITROGEN TETROXIDE

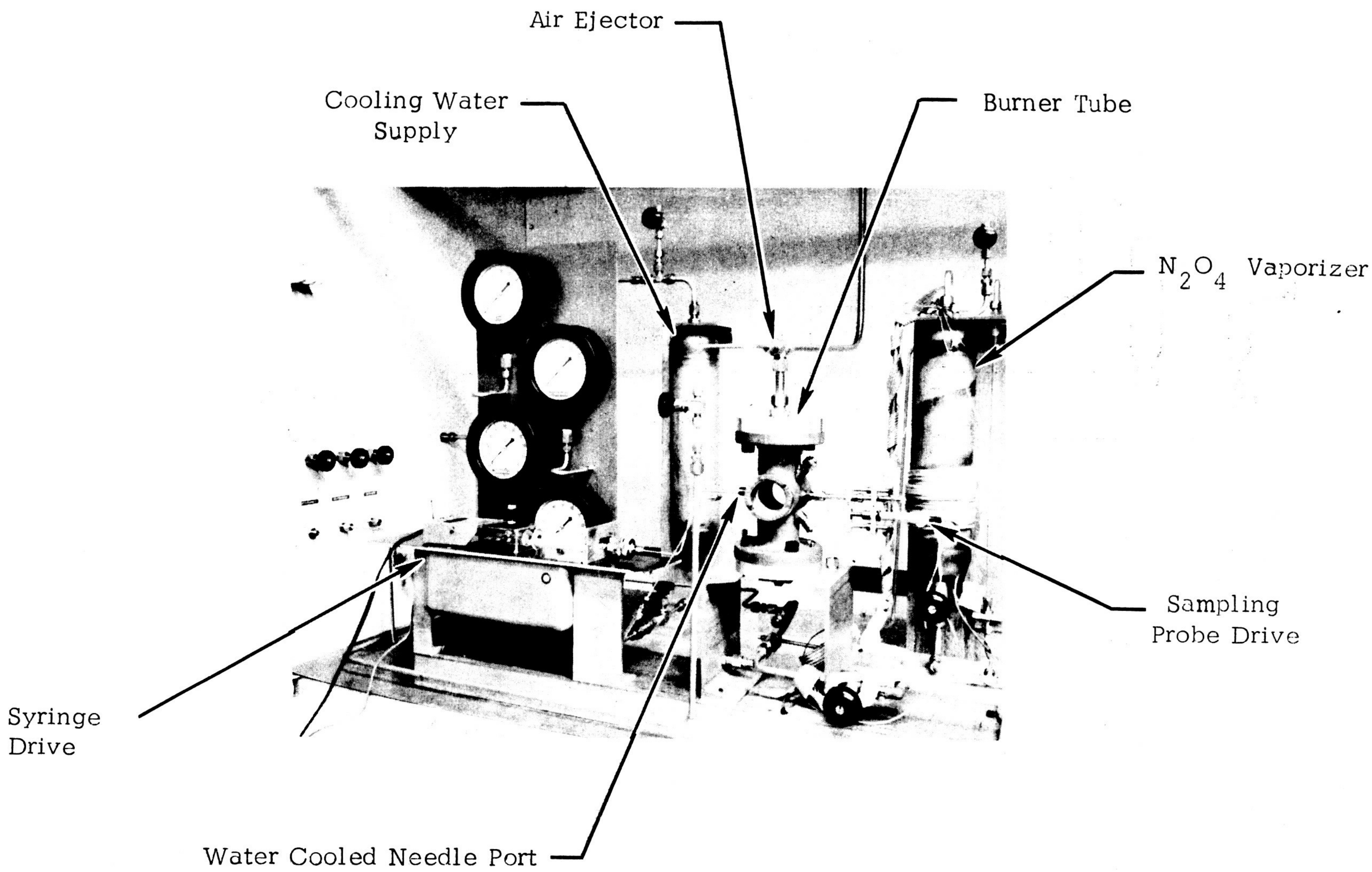

FIGURE 2. HYDRAZINE DROPLET BURNING SETUP.

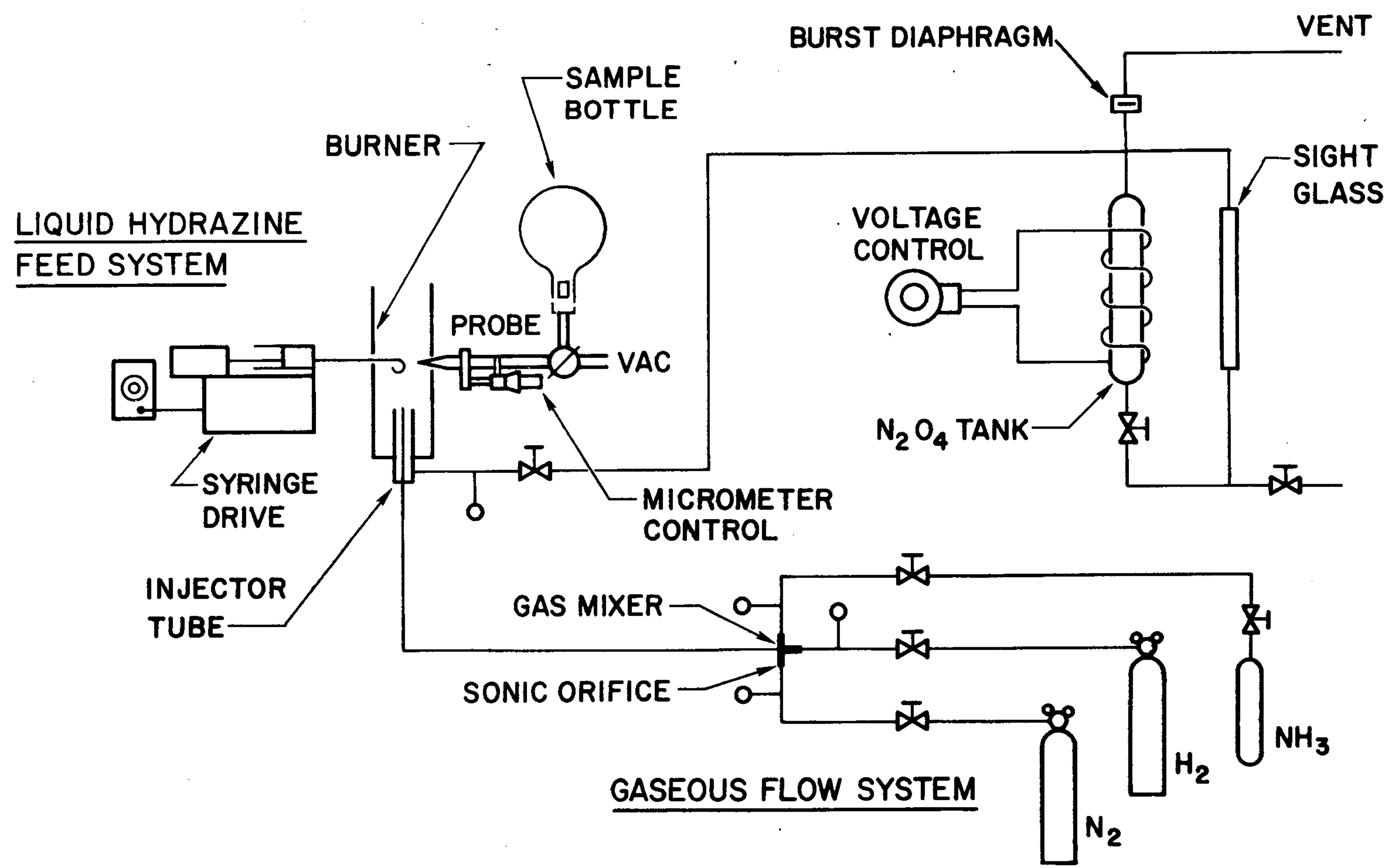

FIGURE 3. N_2H_4/N_2O_4 BURNER

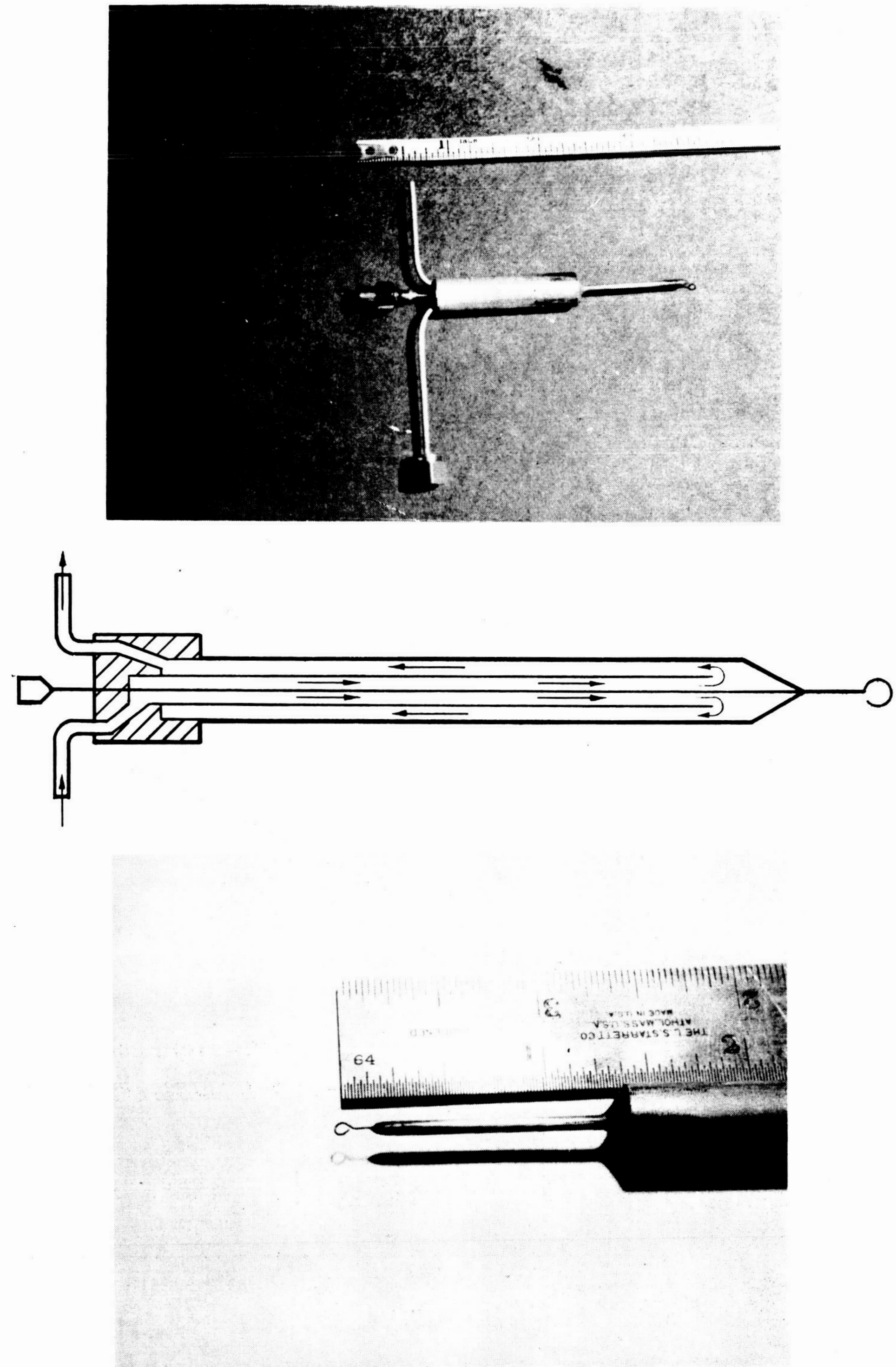

FIGURE 4.   WATER COOLED NEEDLE

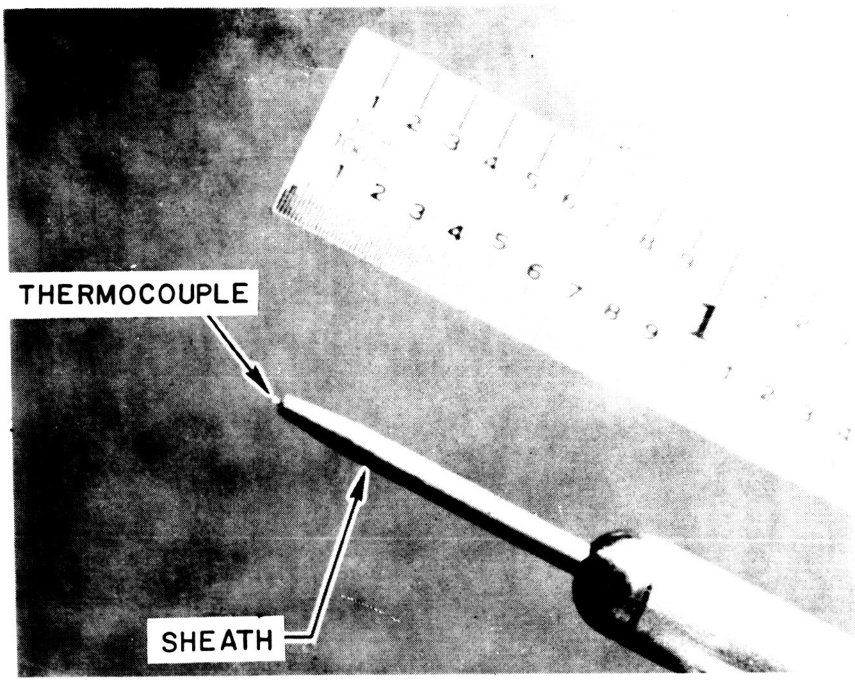

FIGURE 5. TEMPERATURE PROBE

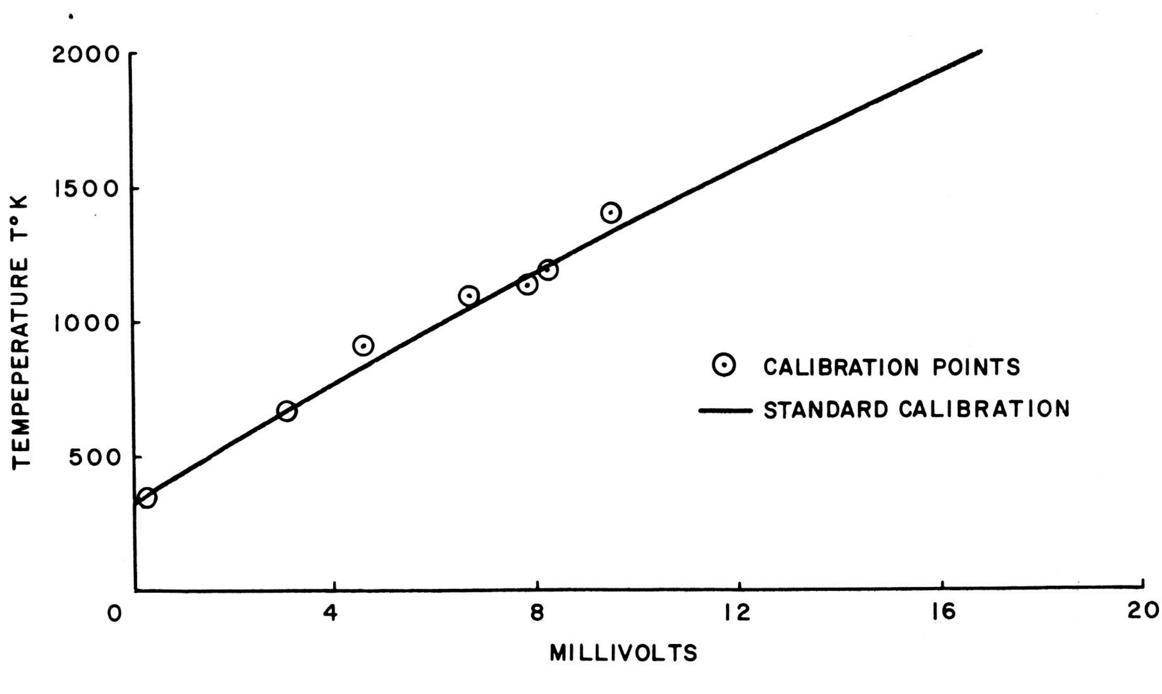

FIGURE 6. THERMOCOUPLE CALIBRATION

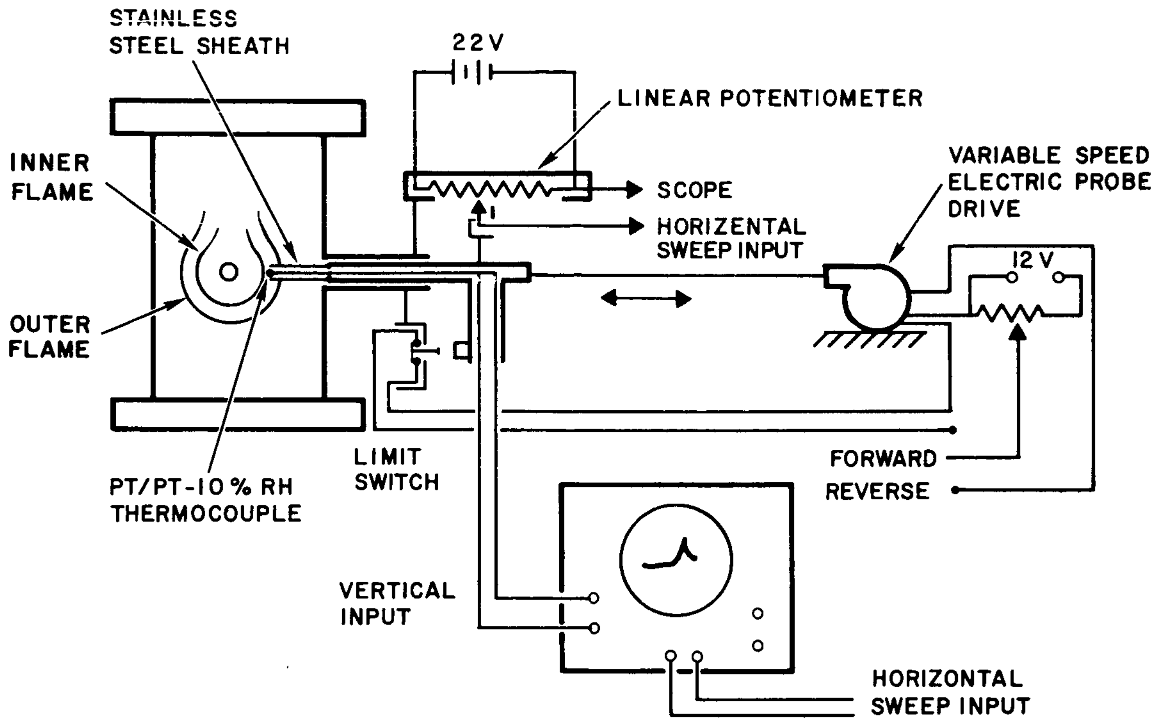

FIGURE 7. THERMOCOUPLE PROBE SETUP

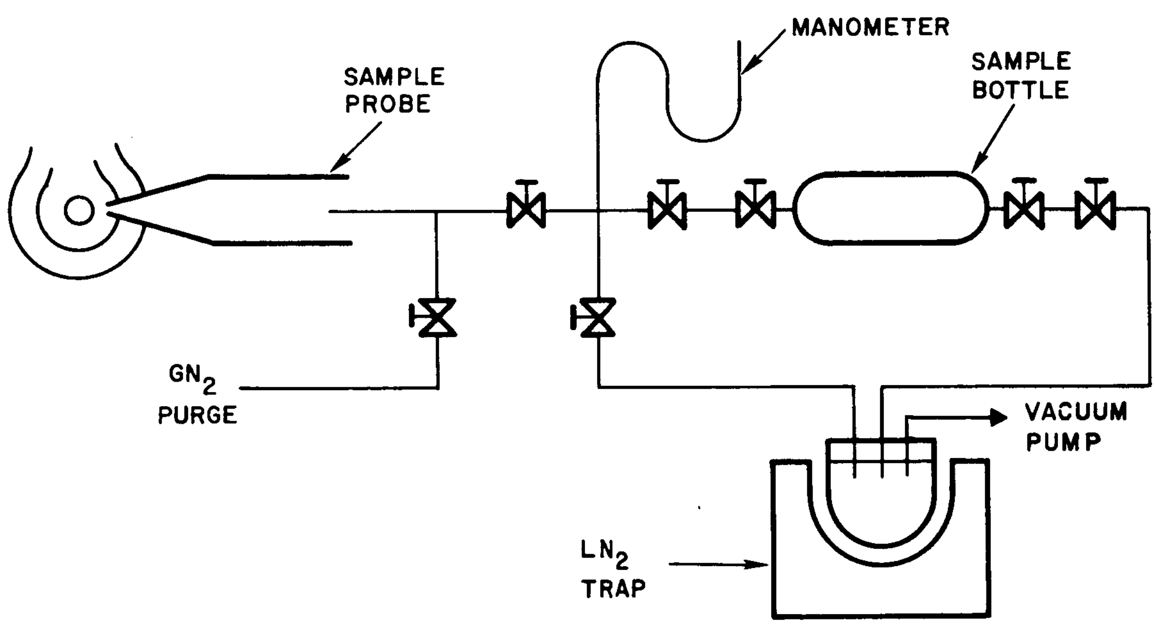

FIGURE 8. FLAME SAMPLING VACUUM SYSTEM

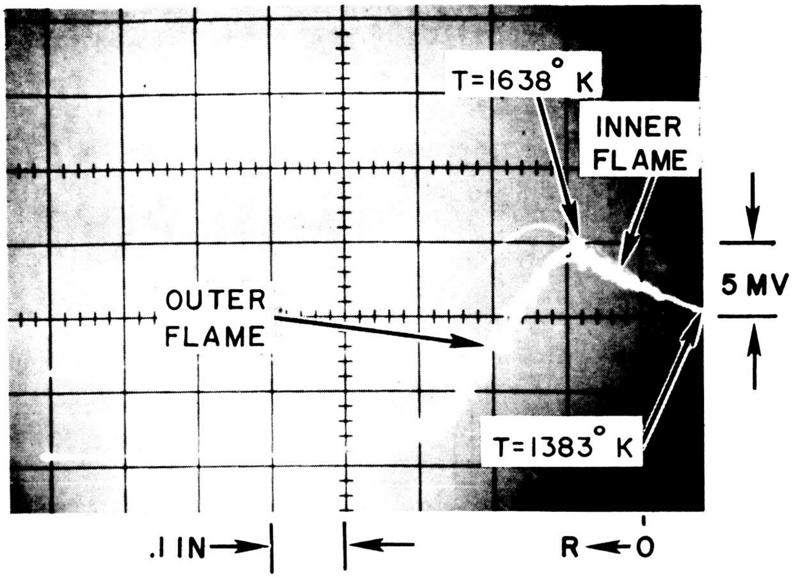

FIGURE 9. HYDRAZINE/NITROGEN TETROXIDE FLAME TEMPERATURE PROFILE

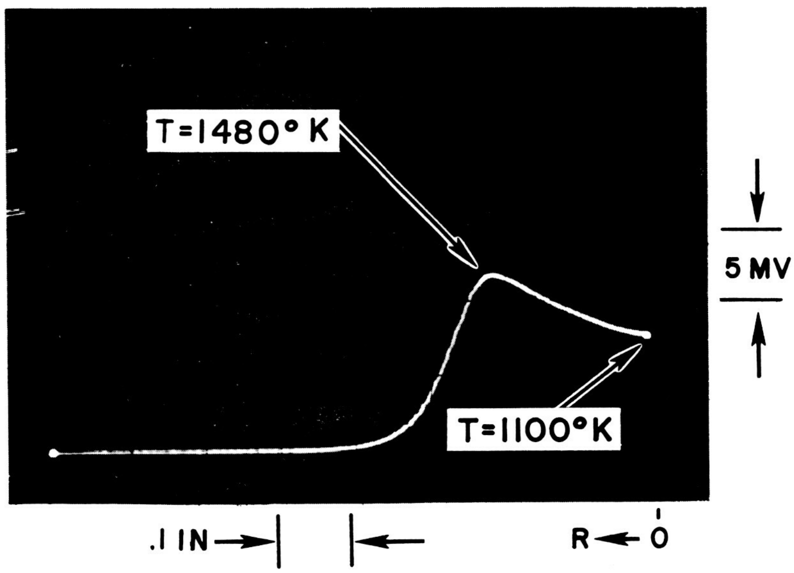

FIGURE 10. HYDRAZINE/AIR FLAME TEMPERATURE PROFILE

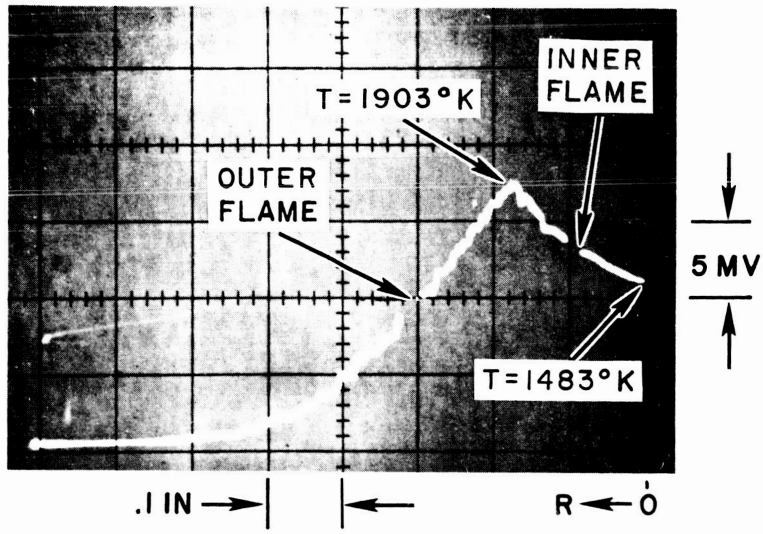

FIGURE 11a. HYDRAZINE - O_2/N_2 FLAME HIGH O_2/N_2 RATIO TEMPERATURE PROFILE

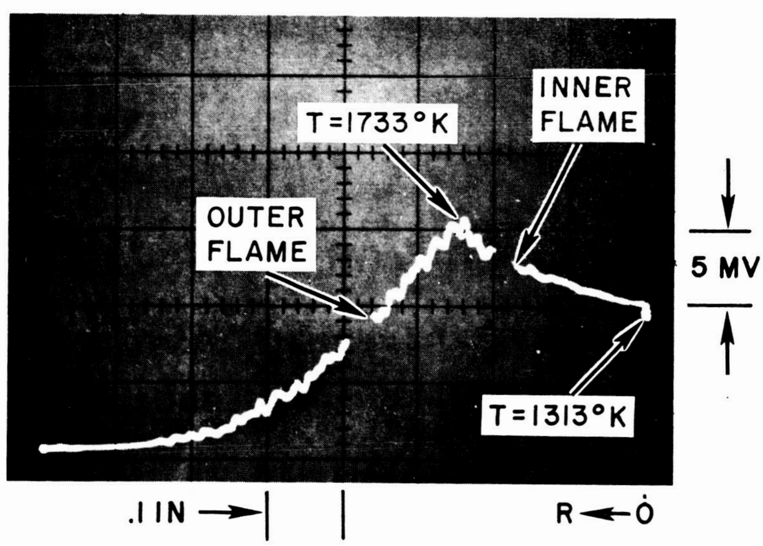

FIGURE 11b. HYDRAZINE - O_2/N_2 FLAME LOW O_2/N_2 RATIO TEMPERATURE PROFILE

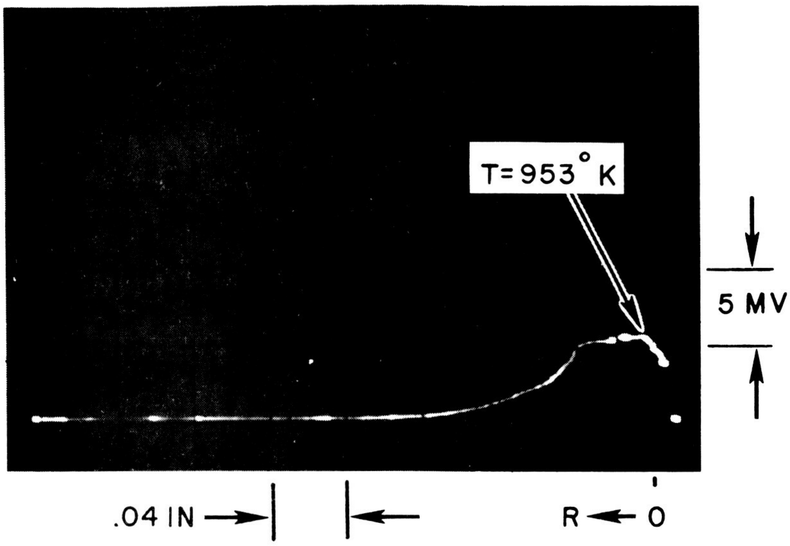

FIGURE 12. HYDRAZINE/LOW OXIDIZER CONCENTRATION TEMPERATURE PROFILE

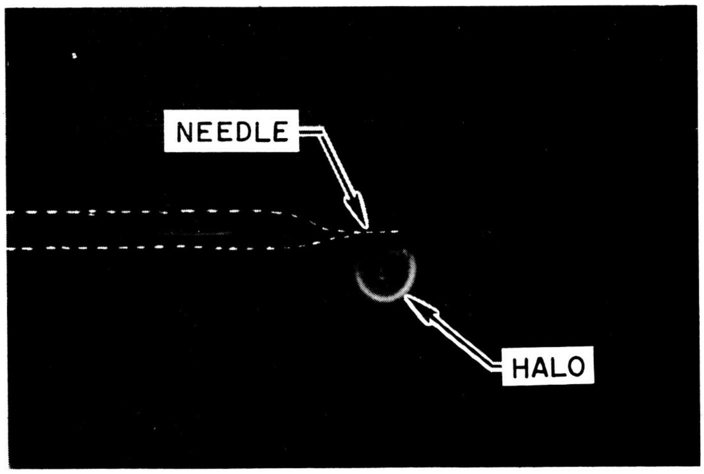

FIGURE 13. HYDRAZINE/LOW OXIDIZER CONCENTRATION HALO

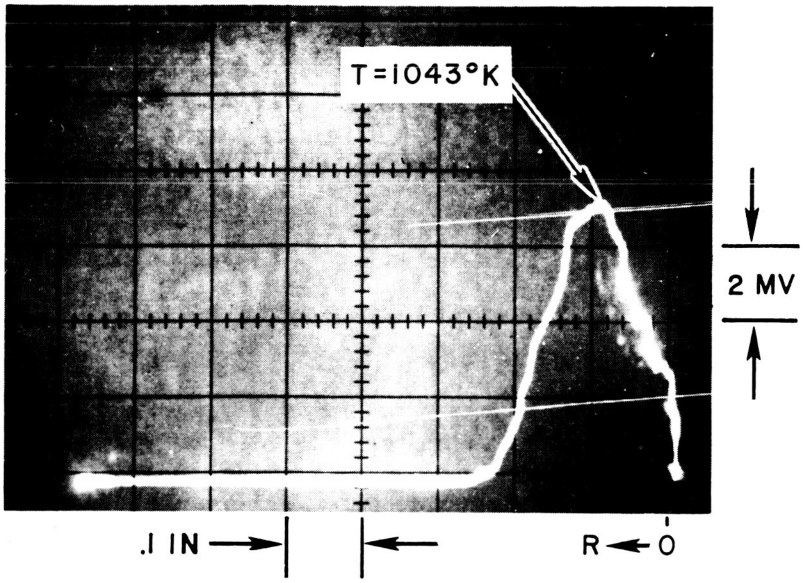

FIGURE 14a. TEMPERATURE PROFILE
HEPTANE/NTO FLAME

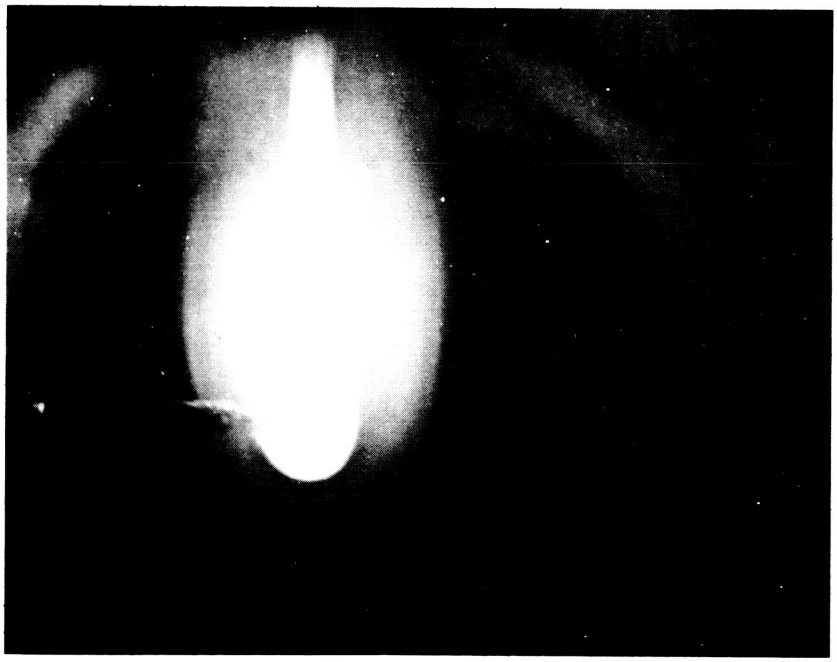

FIGURE 14b. DROPLET FLAME
HEPTANE/NTO FLAME

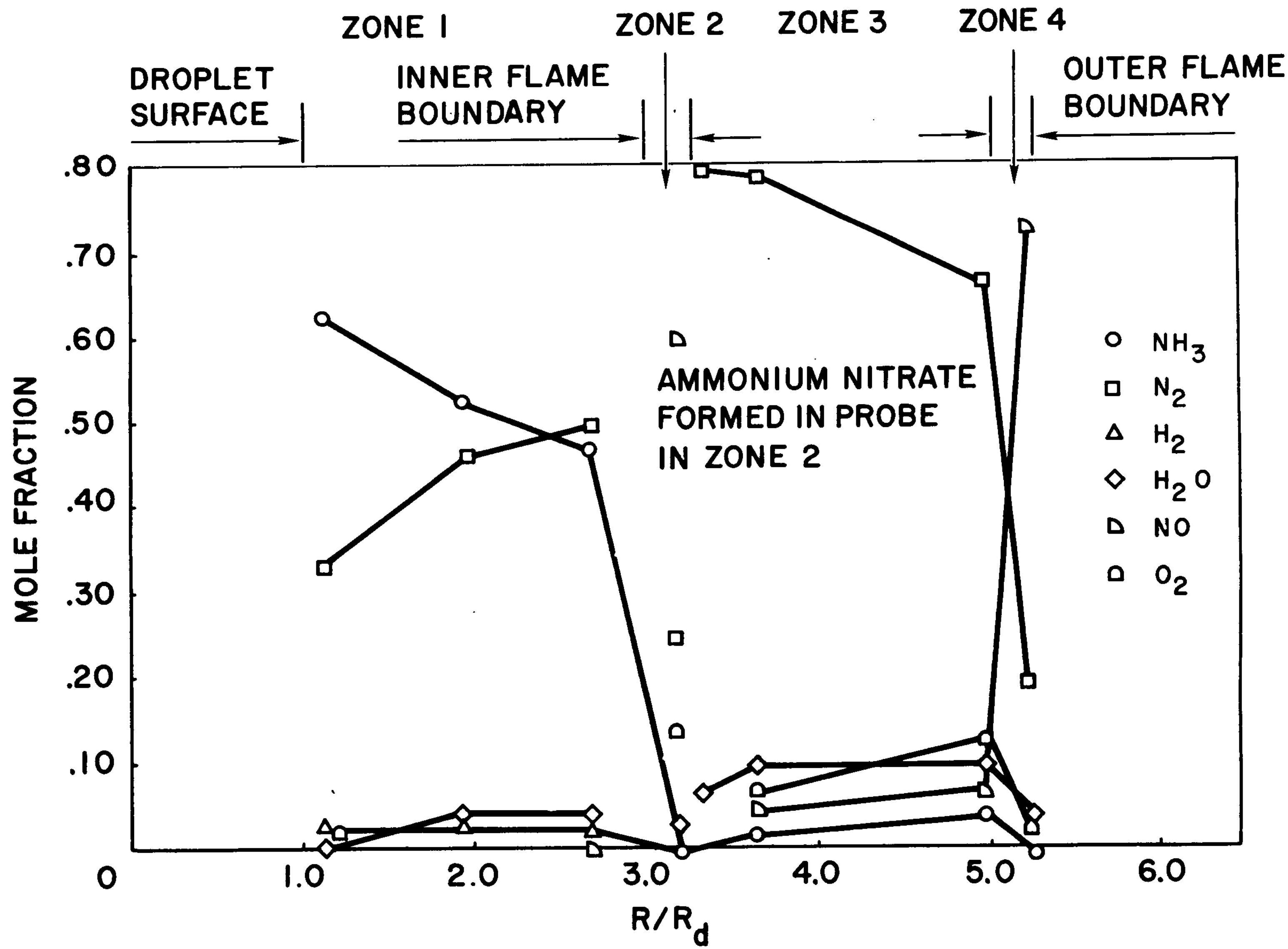

FIGURE 15. CONCENTRATION vs REDUCED RADIUS FOR N_2H_4/NO_2 FLAME

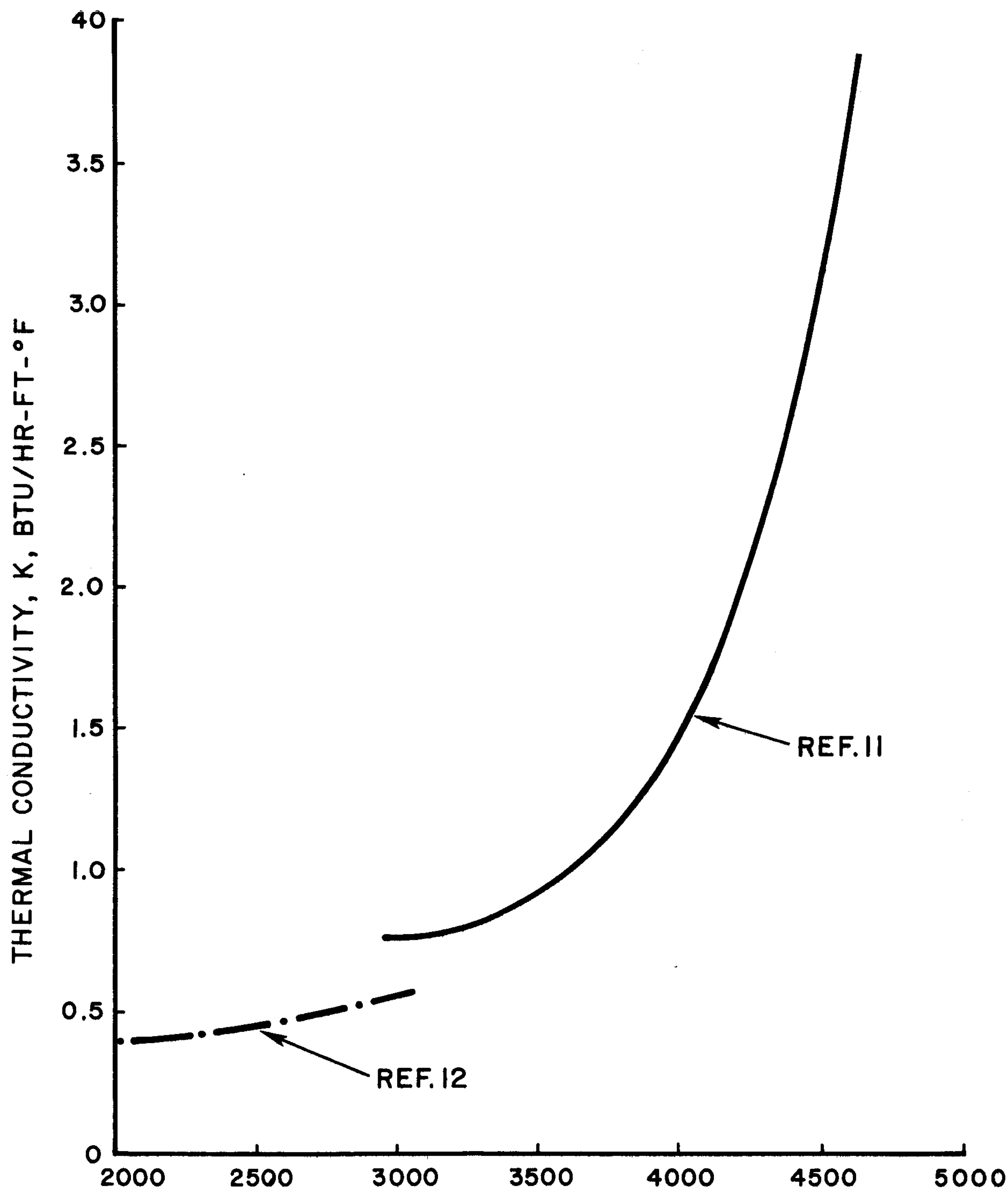

FIGURE 16. HYDROGEN THERMAL CONDUCTIVITY

DISTRIBUTION LIST

NASA Pasadena Office (1)
4800 Oak Grove Drive
Pasadena, California 91103
Patents and Contract Management

Western Support Office (1)
150 Pico Boulevard
Santa Monica, California 90406
Office of Technical Information

Technical Monitor (1)
Mr. Charles Feiler
Lewis Research Center
21000 Brookpark Road
Cleveland, Ohio 44135

Chief, Liquid Propulsion Technology (4)
Code: RPL
Office of Advanced Research & Technology
NASA Headquarters
Washington, D. C. 20546

NASA Scientific and Technical Information Facility (25)
P. O. Box 33
College Park, Maryland 20740

Mr. Vincent L. Johnson (1)
Director, Launch Vehicles and Propulsion
Office of Space Science and Applications
NASA Headquarters
Washington, D. C. 20546

Mr. George S. Trimble (1)
Director, Advanced Manned Missions
Code: MT
Office of Manned Space Flight
NASA Headquarters
Washington, D. C. 20546

Mr. A. Gessow (1)
Chief, Physics of Fluids Branch
Office of Advanced Research and Technology
NASA Headquarters
Washington, D. C. 20546

Mr. Leonard Roberts (1)
Mission Analysis Division
NASA Ames Research Center
Moffett Field, California 24035

Technical Librarian (2)
Ames Research Center
Moffett Field, California 94035

Technical Librarian (2)
Goddard Space Flight Center
Greenbelt, Maryland 20771

Technical Librarian (1)
Jet Propulsion Laboratory
California Institute of Technology
4800 Oak Grove Drive
Pasadena, California 91103

Technical Librarian (2)
Langley Research Center
Langley Station
Hampton, Virginia

Technical Librarian (2)
Lewis Research Center
21000 Brookpark Road
Cleveland, Ohio 44135

Technical Librarian (2)
Marshall Space Flight Center
Huntsville, Alabama 35812

Technical Librarian (2)
Manned Spacecraft Center
Houston, Texas

Technical Librarian (2)
Western Support Office
150 Pico Boulevard
Santa Monica, California 90406

Technical Librarian (2)
John F. Kennedy Space Center, NASA
Kennedy Space Center, Florida 32899

Technical Librarian (1)
Aeronautical System Division
Air Force Systems Command
Wright-Patterson Air Force Base
Dayton, Ohio 45433

Technical Librarian (1)
Air Force Missile Development Center
Holloman Air Force Base
New Mexico, California

Technical Librarian (1)
Air Force Missile Test Center
Patrick Air Force Base, Florida

Technical Librarian (1)
Air Force Systems Division
Air Force Unit Post Office
Los Angeles 45, California

Technical Librarian (1)
Arnold Engineering Development
Center
Arnold Air Force Station
Tullahoma, Tennessee

Technical Librarian (1)
Bureau of Naval Weapons
Department of the Navy
Washington, D. C.

Technical Librarian (1)
Chemistry Research Laboratory
Building 450
Wright-Patterson Air Force Base
Dayton, Ohio 45433

Technical Librarian (1)
Department of the Navy
Office of Naval Research
Washington, D. C. 20360

Technical Librarian (1)
Defense Documentation Center Hdqs.
Cameron Station, Building 5
5010 Duke Street
Alexandria, Virginia 22314

Technical Librarian (1)
Headquarters, U. S. Air Force
Washington, D. C.

Technical Librarian (1)
Headquarters Research and
Technology Division
Air Force Systems Command
Bolling Air Force Base
Washington, D. C. 20332

Technical Librarian (1)
Picatinny Arsenal
Dover, New Jersey 07801

Technical Librarian (1)
Air Force Rocket Propulsion Lab.
Research and Technology Division
Air Force Systems Command
Edwards, California 93523

Technical Librarian (1)
U. S. Atomic Energy Commission
Technical Information Services
Box 62
Oak Ridge, Texas

Technical Librarian (1)
U. S. Army Missile Command
Redstone Arsenal
Huntsville, Alabama 35808

Technical Librarian (2)
U. S. Naval Ordnance Test Station
China Lake, California 93555

Technical Librarian (1)
Air Force Office of Scientific
Research
Propulsion Division
1400 Wilson Blvd.
Arlington, Virginia 22209

Technical Librarian (2)
Chemical Propulsion Information
Agency
Applied Physics Laboratory
8621 Georgia Avenue
Silver Spring, Maryland 20910

Technical Librarian (1)
Aerojet-General Corporation
P. O. Box 296
Azusa, California 91703

Technical Librarian (1)
Aerojet-General Corporation
P. O. Box 15847
Sacramento, California 95809

Technical Librarian (1)
Aeronautronic
Philco Corporation
Ford Road
Newport Beach, California 92663

Technical Librarian (1)
Aerospace Corporation
2400 East El Segundo Boulevard
P. O. Box 95085
Los Angeles, California

Technical Librarian (1)
Astrosystems International, Inc.
1275 Bloomfield Avenue
Fairfield, New Jersey 07007

Technical Librarian (1)
Atlantic Research Corporation
Edsall Road and Shirley Highway
Alexandria, Virginia 23314

Technical Librarian (1)
Beech Aircraft Corporation
Boulder Division
Box 631
Boulder, Colorado

Technical Librarian (1)
Bell Aerosystems Company
P. O. Box 1
Buffalo, New York 14205

Technical Librarian (1)
Bendix Corporation
Bendix Systems Division
3300 Plymouth Road
Ann Arbor, Michigan

Technical Librarian (1)
Boing Company
P. O. Box 3707
Seattle, Washington 98124

Technical Librarian (1)
Chrysler Corporation
Missile Division
P. O. Box 2628
Detroit, Michigan 48231

Technical Librarian (1)
Curtiss-Wright Corporation
Wright Aeronautical Division
Wood-Ridge, New Jersey 07075

Technical Librarian (1)
Dartmouth University
Hanover, New Hampshire 03755

Technical Librarian (1)
Defense Research Corporation
P. O. Box 3587
Santa Barbara, California 93105

Technical Librarian (1)
Douglas Aircraft Company, Inc.
Missile and Space Systems Division
3000 Ocean Park Boulevard
Santa Monica, California 90406

Technical Librarian (1)
Dynamic Science Corporation
1900 Walker Avenue
Monrovia, California 91016

Technical Librarian (1)
Fairchild Hiller Corporation
Aircraft Missiles Division
Hagerstown, Maryland

Technical Librarian (1)
General Dynamics-Astronautics
Library & Information Services
Code: 128-00
P. O. Box 1128
San Diego, California 92112

Technical Librarian (1)
General Electric Company
Re-Entry Systems Department
3198 Chestnut Street
Philadelphia, Pennsylvania 19101

Technical Librarian (1)
General Electric Company
Advanced Engine & Technology Dept.
Cincinnati, Ohio 45215

Technical Librarian (1)
Geophysics Corporation of America
Technical Division
Burlington Road
Bedford, Massachusetts

Technical Librarian (1)
Georgia Institute of Technology
Aerospace School
Atlanta, Georgia 30332

Technical Librarian (1)
Grumman Aircraft Engineering Corp.
Bethpage, Long Island
New York

Technical Librarian (1)
Ling-Temco-Vought Corporation
Astronautics
P. O. Box 5907
Dallas, Texas 75222

Technical Librarian (1)
Arthur D. Little, Inc.
20 Acorn Park
Cambridge, Massachusetts 02140

Technical Librarian (1)
Lockheed California Company
2555 North Hollywood Way
Burbank, California 91503

Technical Librarian (1)
Lockheed Missiles and Space Company
Attn: Technical Information Center
P. O. Box 504
Sunnyvale, California 94088

Technical Librarian (1)
Lockheed Propulsion Company
P. O. Box 111
Redlands, California 92374

Technical Librarian (1)
The Marquardt Corporation
16555 Saticoy Street
Van Nuys, California 91409

Technical Librarian (1)
Martin Marietta Corporation
Baltimore Division
Baltimore, Maryland 21203

Technical Librarian (1)
Martin Marietta Corporation
Denver Division, P.O Box 179
Denver, Colorado 80201

Technical Librarian (1)
Space General Corporation
9200 East Flair Avenue
El Monte, California 91734

Technical Librarian (1)
Stanford Research Institute
333 Ravenswood Avenue
Menlo Park, California 94025

Technical Librarian (1)
TRW Incorporated
TRW Systems Group
One Space Park
Redondo Beach, California 90278

Technical Librarian (1)
Thiokol Chemical Corporation
Huntsville Division
Huntsville, Alabama

Technical Librarian (1)
Thiokol Chemical Corporation
Reaction Motors Division
Denville, New Jersey 07832

Technical Librarian (2)
United Aircraft Corporation
Research Laboratories
400 Main Street
East Hartford, Connecticut 06108

Technical Librarian (1)
United Technology Center
587 Methilda Avenue
P. O. Box 358
Sunnyvale, California 94088

Technical Librarian (1)
University of California
Department of Chemical Engineering
6161 Etcheverry Hall
Berkeley, California 94720

Technical Librarian (1)
University of California
Department of Mechanical Engineering
Thermal Systems
Berkeley, California 94720

Technical Librarian (1)
University of Michigan
Aerospace Engineering
North Campus
Ann Arbor, Michigan 48104

Technical Librarian (1)
University of Southern California
Department of Mechanical Engineering
University Park
Los Angeles, California 90007

Technical Librarian (1)
University of Wisconsin
Department of Mechanical Engineering
1513 University Avenue
Madison, Wisconsin 53705

Technical Librarian (1)
Walter Kidde and Company, Inc.
Aerospace Operations
567 Main Street
Belleville, New Jersey 07109

Technical Librarian (1)
Warner-Swasey Company
Control Instrument Division
32-16 Downing Street
Flushing, New York 11354

Technical Librarian (1)
Rocket Research Corporation
520 South Portland Street
Seattle, Washington 98108

Technical Librarian (1)
Illinois Institute of Technology
3300 S. Federal Street
Chicago, Illinois 60616

Technical Librarian (1)
Massachusetts Institute of Tech.
Department of Mechanical Engineering
Cambridge, Massachusetts 02139

Technical Librarian (1)
McDonald-Douglas Aircraft Company
Astropower Division
2121 Paularino
Newport Beach, California 92663

Technical Librarian (1)
McDonnell Aircraft Corporation
P. O. Box 516
Municipal Airport
St. Louis, Missouri 63166

Technical Librarian (1)
Multi-Tech. Inc.
601 Glenoaks Boulevard
San Fernando, California

Technical Librarian (1)
North American Aviation, Inc.
Space & Information Systems Div.
12214 Lakewood Boulevard
Downey, California 90241

Technical Librarian (1)
North American Aviation, Inc.
ROCKETDYNE
6633 Canoga Avenue
Canoga Park, California 91304

Technical Librarian (1)
Northrop Space Laboratories
3401 West Broadway
Hawthorne, California

Technical Librarian (1)
The Pennsylvania State University
Mechanical Engineering Department
207 Mechanical Engineering Blvd.
University Park, Pennsylvania 16802

Technical Librarian (1)
Polytechnic Institute of Brooklyn
Graduate Center
Route 110
Farmingdale, New York

Technical Librarian (1)
Pratt and Whitney Aircraft
(United Aircraft Corporation)
Florida Research and Development
P. O. Box 2691
West Palm Beach, Florida 33402

Technical Librarian (1)
Princeton University
Forrestal Research Center
Guggenheim Laboratories
Princeton, New Jersey 08540

Technical Librarian (1)
Purdue University
School of Mechanical Engineering
Lafayette, Indiana 47907

Technical Librarian (1)
Ohio State University
Department of Aeronautical &
Astronautical Engineering
Columbus, Ohio 43210

Technical Librarian (1)
Radio Corporation of America
Astro-Electronics Division
Princeton, New Jersey 08540

Technical Librarian (1)
Republic Aviation Corporation
Farmingdale, Long Island
New York

Technical Librarian (1)
Sacramento State College
Engineering Division
60000 J. Street
Sacramento, California 95819

Technical Librarian (1)
Cetec Corporation
188 Whisman Road
Mountain View, California

Technical Librarian (1)
Technology Incorporated
6461 Edsall Road
Alexandria, Virginia 22312